Enabling modular dosage form concepts for individualized multidrug therapy: Expanding the design window for poorly water-soluble drugs

(article starts on next page)

Enabling modular dosage form concepts for individualized multidrug therapy: Expanding the design window for poorly water-soluble drugs

Rydvikha Govender [a,b,*], Susanna Abrahmsén-Alami [a], Staffan Folestad [c], Martina Olsson [d], Anette Larsson [b]

[a] *Oral Product Development, Pharmaceutical Technology and Development, Operations, AstraZeneca, SE-43183 Gothenburg, Sweden*
[b] *Pharmaceutical Technology, Chemistry and Chemical Engineering, Chalmers University of Technology, SE-41296 Gothenburg, Sweden*
[c] *Innovation Strategies and External Liaison, Pharmaceutical Technology and Development, Operations, AstraZeneca, SE-43183 Gothenburg, Sweden*
[d] *Department of Physics, Chalmers University of Technology, SE-41296 Gothenburg, Sweden*

ARTICLE INFO

ABSTRACT

Multidrug dosage forms (aka combination dosage forms, polypills, etc.) create value for patients through reduced pill burdens and simplified administration to improve adherence to therapy. Enhanced flexibility of multidrug dosage forms would provide further opportunities to better match emerging needs for individualized therapy. Through modular dosage form concepts, one approach to satisfy these needs is to adapt multidrug dosage forms to a wider variety of drugs, each with a variety of doses and release profiles. This study investigates and technically explores design requirements for extending the capability of modular multidrug dosage form concepts towards *individualization*. This builds on our recent demonstration of independent tailoring of dose and drug release, which is here extended towards poorly water-soluble drugs. The challenging design requirement of carrying higher drug loads in smaller volumes to accommodate multiple drugs at their clinical dose is here met regarding dose and release performance. With a modular concept, we demonstrate high precision (<5% RSD) in dose and release performance of individual modules containing felodipine or naproxen in Kollidon VA64 at both a wide drug loading range (5% w/w and 50% w/w drug) and a small module size (3.6 mg). In a forward-looking design-based discussion, further requirements are addressed, emphasizing that reproducible individual module performance is predictive of dosage form performance, provided the modules are designed to act independently. Therefore, efforts to incorporate progressively higher drug loads within progressively smaller module volumes will be crucial to extend the design window further towards full flexibility of future dosage forms for individualized multidrug therapy.

1. Introduction

Multidrug therapy may either be administered as discrete dosage forms or as combination dosage forms (also known as polypills). Polypills have existed in research for over a decade, primarily as fixed-dose combinations intended to reduce pill burdens, simplify regimens, and promote adherence (Bangalore et al., 2007; Demiri et al., 2018; Fernandez-Garcia et al., 2020; Pereira et al., 2020b; Robles-Martinez et al., 2019; Rosenthal and Gavras, 2006). However, whilst such multidrug dosage forms are advantageous for convenient delivery of multidrug therapy, they are not currently designed for *individualized* multidrug therapy. Individualized multidrug therapy in an extensively heterogeneous patient population requires multidrug dosage forms to be available in sufficiently high variety to facilitate tailoring to individual patient needs (Govender et al., 2020b; Srai et al., 2015; Wilson, 2016). This includes an increased variety of unit dose strengths (Deng et al., 2017; Ferrendelli, 2001; Govender et al., 2019, 2020b; Nidanapu et al., 2016; Pouplin et al., 2014; Wening and Breitkreutz, 2011) and an increased variety of drug release profiles (Bhatia et al., 2014; Effinger et al., 2019; Govender et al., 2020a; Govender et al., 2020b; Hens et al.,

---

2017; Khaled et al., 2015a; McConnell et al., 2008) for each active pharmaceutical ingredient (API) in the dosage form. Furthermore, for individualized multidrug therapy, tailoring to varying APIs in patients' varying therapeutic regimens is warranted. Although fixed-dose combination products are not typically designed for variety provision or enhanced flexibility in each of its components, recently, research on flexible-dose products (Fuenmayor et al., 2019; Laukamp et al., 2016; Sadia et al., 2018; Wilson, 2016) and products with flexible drug release profiles (Genina et al., 2017; Khaled et al., 2015a,b; Pereira et al., 2020b; Smeets et al., 2020) have emerged. However, interdependencies between the size, dose, and drug release remain, typically resulting in flexibility in only one product feature at a time. Multifunctional individualization, i.e., the simultaneous and independent tailoring of multiple product features (Govender et al., 2020a; Govender et al., 2020b), e.g. dose and drug release within an acceptable dosage form size, is crucial to enable holistic individualization without compromising handling and swallowability (Drumond and Stegemann, 2020; Meltzer et al., 2006; Messina et al., 2015; Page et al., 2016; Ranmal et al., 2016; Stegemann et al., 2012). Therefore, enabling multifunctional individualization across a broad variety of APIs is an important goal for multidrug dosage forms and the core focus of this study. This serves to enable a greater variety of API combinations through interchangeability of each API and its respective dose and drug release, when required. To the authors' knowledge, the conditions which enable multifunctional individualization across a wide variety of APIs for multidrug dosage forms have not yet been elucidated. Specifically, demonstrating opportunities for interchangeability between APIs of varying physicochemical characteristics in the multidrug dosage form, whilst individualizing the dose and drug release of each constituent API, are few (Pereira et al., 2019; Pereira et al., 2020a) and still lack the dose–size independence that is critical to multifunctional individualization.

To address this challenge, we position this study in the context of modular multidrug dosage forms with a high degree of modularity (i.e. more modules in a product). Non-modular multidrug dosage forms, containing a mixture of APIs in a common matrix, rely on compatibility between constituent APIs and do not satisfy the requirement for independent control of product attributes for individualization. A high degree of product modularity is assumed in this study to extend applicability of future multidrug dosage forms to individualized multidrug therapy. In reality, the required degree of modularity for individualization will depend, in part, on the extent of variability in the patient population for a particular API and how that variability translates to health outcomes when treated with a particular product variant.

It has been demonstrated previously that enhanced product variety can be achieved by reconfigurable assembly of unique functional modules into a final dosage form of predefined individualized performance (Siiskonen et al., 2018; Govender et al., 2020a). A higher degree of product modularity theoretically corresponds to a higher product variety using reconfiguration (Gershenson et al., 1999; Ulrich and Tung, 1991) and is therefore desirable for individualized multidrug therapy. Typical multidrug dosage forms with a low degree of modularity and fixed assembly of unique API modules into final dosage forms do not support enhanced variety through reconfiguration or multifunctional individualization. For example, modular fixed-dose combinations are modular only with respect to the APIs but not with respect to each API's dose and drug release (Baumgartner et al., 2020; Fernandez-Garcia et al., 2020).

Current polypill research involves plentiful demonstrations of assembled polypills (Acosta-Vélez et al., 2018; Fernandez-Garcia et al., 2020; Genina et al., 2017; Khaled et al., 2015a; Pereira et al., 2019; Pereira et al., 2020a; Robles-Martinez et al., 2019; Sadia et al., 2018). Importantly, the performance of assembled modular multidrug dosage forms is determined by the performance of the individual modules from which the dosage form is constructed, provided the modules are designed to act independently to meet the requirements for multifunctional individualization. Nevertheless, scrutinizing individual module performance and how it can contribute to extending the applicability of multidrug dosage forms towards individualized multidrug therapy is inadequately addressed to date. In response, this study focuses on the performance of individual modules for future application in assembling modular multidrug dosage forms with a high degree of modularity (Fig. 1).

A higher degree of modularity for individualized multidrug therapy requires not only progressively smaller modules but reproducible and robust dose and release performance at low and high drug loads at these small module sizes, for a variety of APIs. This is the key technical challenge for enabling individualized multidrug therapy and provides the rationale for the study focus on individual module performance instead of assembly of modules or fabrication of polypills. This study aims to delineate the current design window regarding the applicability of flexible combination dosage forms to APIs of varying characteristics, with a focus on APIs with poor aqueous solubility formulated as amorphous solid dispersions.

The properties of the APIs, specifically the recrystallization tendency and dose: solubility ratio, are hypothesized to influence single-module performance, potentially limiting the applicability of multidrug dosage forms for individualized multidrug therapy to drugs with a low dose and low recrystallization tendency. In this study, this challenge is addressed by, firstly, demonstrating the effect of drug loading (5% w/w vs. 50% w/w drug) and recrystallization tendency on the variability in the dose fraction and drug release kinetics between individual drug-containing modules and, thereafter, elucidating the impact of these findings on the feasibility of multidrug dosage forms for individualized multidrug therapy for a broad variety of APIs. Compositions, manufacturing processes, and test parameters were deliberately selected to isolate the effect of the API properties of interest in this study. The potential of the inherent recrystallization tendency of each API to result in recrystallization during dissolution, not recrystallization during storage, was specifically studied. Translating learnings from model systems to real therapeutic solutions will require considerations of added complexity from storage conditions and duration (which may influence solid state properties and stability), manufacturing and dispensing of individual modules at varying length scales, and progression towards more bio-relevant test conditions. However, for future assembly of modules into final dosage forms, the time scales of storage and the conditions under which storage may occur are not yet established. Therefore, stability testing under varying storage conditions is out of scope in this study.

2. Materials and methods

2.1. Materials

Felodipine (FEL) and naproxen (NAP) were selected as model drugs because they span extremes of dose (and dose: solubility ratios) and recrystallization tendencies. FEL (MW 384.3 g/mol) was obtained from AstraZeneca, Sweden. NAP (MW 230.3 g/mol) was purchased from MP Biomedicals, Illkirch, France. VA64 (Kollidon® VA64) was supplied by BASF, Ludwigshafen, Germany. Sodium dodecyl sulphate (SDS) and hydrochloric acid (HCl, 37%) were purchased from Sigma Aldrich, Sweden. FEL is classified as a glass-forming ability (GFA) class 3 drug with an inherently lower tendency to recrystallize from amorphous form (Alhalaweh et al., 2014; Kawakami, 2019; Konno and Taylor, 2006; Panini et al., 2019) and a lower daily dose range (typical adult dose range 2.5–10 mg) compared to NAP, which is in GFA class 1 with a higher tendency to recrystallize (Alhalaweh et al., 2014; Kawakami, 2019; Liu et al., 2017) and a higher daily dose range for tablets (typical adult daily dose range for NAP tablets ~ 500–1000 mg). This model drug selection allowed a common carrier, vinylpyrrolidone-vinyl acetate copolymer (VA64) to be used in both systems.
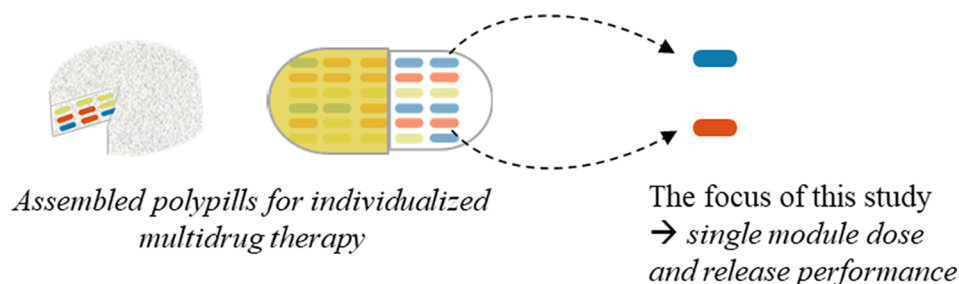
Fig. 1. The focus of this study on individual module dose and release performance for future application as assembled polypills for individualized multidrug therapy (exemplified in the figure).

2.2. Methods

2.2.1. Melt extrusion of drug-containing filaments

Hot melt extrusion (HME) of FEL in VA64 and NAP in VA64 has been shown to solubilize higher drug loads than alternative processing methods, such as spray drying and cryo-milling, during the formation of amorphous solid dispersions (Dedroog et al., 2019; Song et al., 2013). Consequently, four compositions were prepared by HME, namely 5% w/w FEL in VA64, 50% w/w FEL in VA64, 5% w/w NAP in VA64, and 50% w/w NAP in VA64. They are designated FEL5, FEL50, NAP5, and NAP50, respectively, throughout the manuscript. HME was selected to obtain amorphous solid dispersions for solubility enhancement of both APIs as well as to obtain a homogeneous distribution of the drugs in the VA64 through HME's dispersive and distributive mixing. The upper limit for drug load at 50% w/w API was based on the maximum amount of drug that could be solubilized in VA64 during HME allowing the formulation to remain amorphous in the solid state for subsequent drug release testing. The minimum drug load of 5% w/w API represents reference formulations, which were required to elucidate the impact of drug loading on individual module performance. The selection of VA64 was based on its ability to solubilize both drugs at the drug loading range of interest in the solid state (Lu et al., 2019; Sarpal et al., 2019), thereby allowing discrimination of the role of the API on dose and release performance in modular dosage forms. For each composition, VA64 powder, together with either FEL powder or NAP powder, was weighed in a weigh boat in an approximately 5 g batch size and mixed with a spatula until homogeneous upon visual inspection. Physical mixtures were fed via a hopper into the barrel of a 5 mL capacity Xplore micro compounder (Xplore, The Netherlands), affixed with conical mixing screws and a circular die, 1.5 mm in diameter. Both FEL-containing and NAP-containing formulations were fed into a barrel set at 100 °C. This was below the glass transition temperature (T_g) of pure VA64 which prevented sticking and bridging of the powdered polymer in the hopper. After complete feeding (<2 min), the barrel temperature was increased to 150 °C for FEL-containing formulations and 160 °C for NAP-containing formulations, at which temperatures the mixtures were recirculated for 10 min to aid homogenization prior to extrusion through the die to obtain cylindrical filaments, which were allowed to cool at room temperature. These processing temperatures were above the melting temperatures (T_m) of the pure drugs and below the degradation temperatures of all components (229 °C for FEL, 236 °C for NAP, and 292 °C for VA64), as determined by the thermogravimetric analysis (TGA) method described in 2.2.3. Ejection required a reduction in barrel temperature to 115 °C for the formulations containing 50% w/w drug to allow an increase in ejection force. A constant screw speed of 50 rpm was maintained throughout feeding, recirculation, and ejection. Filaments were stored for 1–3 days post-extrusion in sealed plastic bags at room temperature prior to further processing. The physical stability of these model systems under varying conditions and durations has been studied previously (Lehmkemper et al., 2018, Song, et al., 2013).

2.2.2. Sectioning of melt-extruded filaments into target module size

Melt-extruded filaments were cut into sections with a blade on the same day as the drug release testing was to be conducted. These filament sections represent the modules that were used in in vitro drug release testing immediately after sectioning. The nominal module size for the standard-size (small) modules was set at 3.5 mg. This was based on the minimum module size that could be reproducibly generated from the extruded filament across formulations and satisfy the volumetric constraints of the drug release testing method. Larger modules of 7 mg were also prepared for some of the release experiments described below. All modules were obtained from different regions along the length of the extruded filament. Individual modules from FEL5, FEL50, NAP5, and NAP50 were weighed in a Mettler MT5 analytical balance (Mettler Toledo, Greifensee, Zurich, Switzerland) and module dimensions were measured using a digital caliper.

2.2.3. Thermal characterization

To determine the onset of thermal degradation of raw materials (T_{deg}), TGA was performed on FEL, NAP, and VA64 powders using a TGA/DSC 3 + STARe system instrument (Mettler Toledo, Switzerland). These powders were weighed in open 70 μL aluminium crucibles using the built-in TGA balance and heated from 30 °C to 500 °C at 10 °C/min under a nitrogen atmosphere with a 50 mL/min flow rate. T_{deg} was reported from the weight vs. temperature curve as the first observed mass loss from the initial baseline in the absence of water loss. In order to facilitate comparison between drugs with different recrystallization tendencies during dissolution, differential scanning calorimetry (DSC) in a DSC 2 STARe system instrument (Mettler Toledo, Switzerland) was first performed to ensure an absence of crystallinity in melt-extruded formulations in the solid state. Melt-extruded filaments and raw materials were weighed separately in 40 μL aluminium crucibles and sealed with aluminium lids with a pinhole. The instrument was run in a heat-cool-heat cycle at 10 °C/min under a 100 mL/min nitrogen atmosphere for all samples (heating from 25 °C to 220 °C, cooling to −50 °C and reheating to 220 °C for FEL-containing samples and heating from 25 °C to 200 °C, cooling to −50 °C and reheating to 200 °C for NAP-containing samples). STARe software (version 16.00b, Mettler Toledo, Greifensee, Zurich, Switzerland) was used for instrument control and thermogram analysis. DSC was run on the same day as each drug release test to ensure the absence of crystallinity in the samples in the solid state prior to commencement of the drug release test. T_g was reported as the midpoint of the T_g range and T_m, if present, was reported as the peak of the melting endotherm.

2.2.4. Wide angle X-ray scattering (WAXS)

A non-destructive analytical method, WAXS, was also used to confirm the absence of crystallinity in the melt-extruded filaments from which the modules for drug release testing were obtained. The filaments were analyzed intact through the bulk of the sample perpendicular to the direction of extrusion using a Mat: Nordic X-Ray scattering instrument (SAXSLAB, Copenhagen, Denmark) equipped with a high brilliance Rigaku 003 X-Ray micro-focus Cu-radiation source (Rigaku

Innovative Technologies Inc., Michigan, United States) and a Pilatus 300 K detector (Dectris, Baden-Daettwil, Switzerland). Samples were analyzed in a vacuum at room temperature with an exposure time of 300 s, beam size of 0.9 mm, and a sample-to-detector distance of 134 mm. The scattering data was collected in the form of a 2D diffraction pattern and the 2D detector intensity was then radially integrated to produce the scattering curve. Ganesha Interactive Control Center (GICC) software (SAXSLAB, Copenhagen, Denmark) was used for instrument operation and the graphical user interface SAXSGUI (Rigaku Innovative Technologies Inc., Michigan, United States and JJ X-Ray Systems ApS., Hoersholm, Denmark) was used for integration from the 2D detector scattering patterns to the resulting 1D curves.

2.2.5. In vitro drug release and drug content homogeneity

In vitro drug release testing was performed on all formulations. Unlike FEL, NAP has a pH-dependent solubility, therefore all experiments were conducted in 0.1 M HCl (pH = 1.4) containing 50 mM SDS, where NAP has poor aqueous solubility. For comparison purposes, selected samples were also evaluated without SDS under non-sink conditions. Sink indices were calculated and reported as

$$SI = Cs/(Dose/V)$$

where C_s is the equilibrium solubility of the drug at 37 °C in the dissolution medium and V is the volume of the dissolution medium (Sun et al., 2016). Volumes of interest for the entire study spanned two orders of magnitude between 7 mL and 900 mL to account for the varying dose: solubility ratios of FEL and NAP and provide an equivalent sink index under non-sink conditions of ~ 0.5 calculated as above. Consequently, for volumes 100 mL and higher (i.e. FEL5 and FEL50), the test was carried out in a USP 2 dissolution apparatus (Varian 705-DS, Agilent Technologies, California, USA) and for samples less than 100 mL (NAP5 and NAP50), a modified USP 1 setup was used, which replaced the large-capacity vessels with small 50 mL or 100 mL glass beakers, each suspended at an equivalent height from the bottom of the rotating basket. All beakers used in a specific test were identical in diameter. In the case of the USP 2 setup, the samples were suspended in the medium and immediately sank to the bottom of the vessel, whereas for the modified USP 1 setup, the samples were housed in the rotating basket. Dissolution apparatuses were operated at 37 ± 1 °C, 50 rpm. Vessel temperature was verified before sample insertion, i.e., before the commencement of each test. At predefined timepoints, 1 mL aliquots of media were withdrawn with fresh media replacement. Withdrawn aliquots were analyzed by ultraviolet (UV) absorbance spectroscopy using a Cary60 UV–Vis spectrophotometer (Agilent Technologies, Inc., CA, USA). Cary WinUV scan application software (version 5.0.0.999, Agilent Technologies, Inc., CA, USA) was used for instrument operation and acquisition of spectra. All sample solutions were scanned at 4800 nm/min from 800 nm to 290 nm for FEL-containing sample solutions and 800 nm to 200 nm for NAP-containing sample solutions. Lower wavelengths were excluded for FEL due to potential photodegradation of FEL at these wavelengths (De Luca et al., 2019; Pizarro et al., 2007). FEL and NAP concentrations were quantified from sample absorbance at 365 nm and 273 nm, respectively and from a calibration curve of drug-containing standards (concentration range 1–10 μg/mL). Linearity was confirmed over this concentration range. Absorbance readings corresponding to greater than or equal to the limit of quantification (signal: noise > 10) were reported. Drug content was quantified from the 100% release timepoint for modules obtained from different sections along the length of the extruded filament and compared to the theoretical individual module drug content.

3. Results

3.1. Confirmation of absence of crystallinity in the solid State: DSC

Fig. 2A and 2B show thermal transitions of raw materials (FEL, NAP) and melt-extruded filaments (FEL5, FEL50, NAP5, NAP50, and VA64) during the first heat cycle. The first heat cycle elucidates the effect of the melt extrusion processing conditions on the solid state of the API in the resulting melt-extruded filaments.

Crystalline FEL powder and crystalline NAP powder displayed melting endotherms at 150.2 °C and 157.4 °C, respectively (T_m, midpoint), which are in approximate agreement with those reported in literature (Chen et al., 2018; Dedroog et al., 2019; Guo et al., 2020; Kawakami, 2019; Liu et al., 2017; Lu et al., 2019). The absence of endothermic peaks for both FEL5 and FEL50 filaments in the region of the pure FEL melting peak (red band in Fig. 2A) confirms an absence of crystallinity in these compositions. VA64 is established as a polymer with a good ability to solubilize and stabilize FEL in the solid state, rationalizing its selection in this study (Song et al., 2013). In fact, previous studies on melt extruded FEL in VA64 filaments revealed that drug loads up to 70% w/w could be achieved in the filaments without crystalline phase separation (Lu et al., 2019; Sarpal et al., 2019). Fig. 2B shows that NAP5 and NAP50 also exhibited an absence of crystallinity in the solid state, analogous to what has been reported previously (Dedroog et al., 2019). The small endotherm at ~ 42 °C for NAP50 corresponds to enthalpic relaxation, which is typically observed towards the end of the T_g range post-extrusion. Processing both formulations above the melting temperature of the APIs during melt extrusion was chosen to enable improved solubilization and miscibility of the APIs in VA64 (Dedroog et al., 2019; Palazi et al., 2018). Due to the choice of polymeric carrier and process conditions, both drugs were able to form crystal-free extrudates at 5% w/w and 50% w/w. VA64 displayed a broad water loss endotherm during the first heat cycle due to the hygroscopicity of the polymer (Maddineni et al., 2015; Song et al., 2013), which masked the glass transition temperature. This was corroborated as a mass loss during TGA (Appendix A, Figure A1). Consequently, the T_g
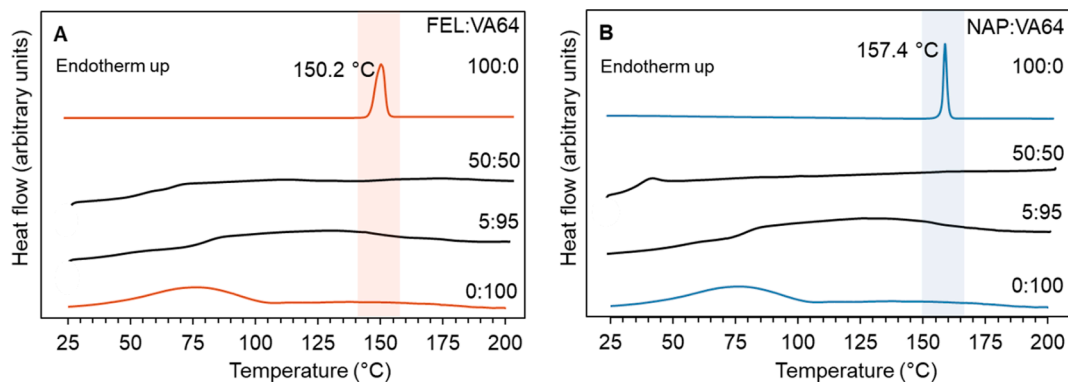

Fig. 2. DSC thermal transitions of (A) FEL and VA64 (red traces), FEL5 and FEL50 (black traces); (B) NAP and VA64 (blue traces), NAP5 and NAP50 (black traces) in heat cycle 1, endotherms point upwards.

was determined from the second heat cycle at approximately 108 °C (T$_g$, midpoint). Since the presence of moisture in melt-extruded filaments may hinder accurate reporting of the T$_g$ in the first heat cycle, the reader is referred to Appendix A (Figure A2) for T$_g$ determination during the second heat cycle. Subsequent release testing relied upon an absence of crystallinity in the solid state to isolate recrystallization during dissolution as a contributor to variability in drug release kinetics of individual modules. Consequently, according to these DSC results, all formulations could be used in subsequent drug release testing.

3.2. Confirmation of absence of crystallinity in the solid state: WAXS

To corroborate the absence of crystallinity revealed during DSC, a second analytical method, WAXS, was used. Pure FEL (Fig. 3A, top trace) and pure NAP (Fig. 3B, top trace) showed sharp, intense peaks in the WAXS curve, characteristic of crystalline materials.

In contrast, VA64, FEL5, FEL50, NAP5, and NAP50, showed broad peaks distributed over a wide 2θ range, which are characteristically ascribed to amorphous materials. Therefore, analogous to the DSC findings, WAXS curves confirmed an absence of crystallinity in all formulations.

3.3. Individual module precision in mass, dimensions, and drug content

To isolate the influence of drug recrystallization tendency during dissolution on variability in release kinetics of individual modules, precision in individual module mass and dose fraction was critical. Fig. 4A and 4B show mean mass and volume, respectively, of small and large modules investigated in subsequent drug release testing. The small modules were FEL5, FEL50, and NAP50 whereas the large modules were NAP5 and NAP50. NAP50 was fabricated as both small and large modules to facilitate comparison between small and large module performance at a high drug load.

Module volumes were calculated based on measured heights and diameters of the cylindrical sections cut from melt-extruded filaments. Fig. 4A and 4B show that % RSD in mass and volume were within an acceptable 5% RSD for modules of both sizes. This reflects not only precise sectioning of individual modules but also that consistent extrudate diameters were obtained from the extruder die. Composition did not affect precision at each module size. Fig. 4C shows that drug content in individual modules were within 5% RSD of each other for 5% w/w and 50% w/w drug loads and within 5% RSD of their target contents.

This was measured by UV absorbance spectroscopy, where dissolved melt-extruded modules displayed the same λ$_{max}$ as standard solutions of dissolved pure drug. Since these modules were obtained from different sections along the length of the filament, this indicates homogeneity in drug distribution in the filaments on a relevant length scale for the module sections chosen for subsequent drug release testing. Despite NAP50 showing slightly more variability in drug content (within 5% RSD) compared to FEL50 (within 1.5% RSD), phase separation was not detected as a second T$_g$ during DSC (Fig. 2B) and precision is within acceptable limits. With precision in mass, dimensions, and drug content established, all modules could be investigated for the contribution of FEL and NAP to variability in drug release kinetics.

3.4. Individual module variability in in vitro drug release kinetics

In vitro drug release testing was performed in 0.1 M HCl containing 50 mM SDS to evaluate variability in drug release kinetics (amount of drug released at each sampling time point) from individual cylindrical modules of predefined size (3.6 mg small modules and 7 mg large modules). The NAP systems were evaluated at a larger size (7 mg) than the FEL systems (3.6 mg) due to the volumetric constraints of the test method, which prevented evaluation of smaller module sizes at low NAP loads. Modular dosage forms enable individualization by reconfigurable assembly, i.e., combining modules with varying drug loads and/or drug release profiles to generate final dosage forms of predictable and predefined performance. To do so, the variability in dose and drug release kinetics between modules of the same composition should be as low as possible. Consequently, release performance is evaluated by comparison of variability in release kinetics between modules of the same composition in the same test, not comparison between release profiles of different modules. The latter would require optimization when translating model systems to applicability for real target indications. FEL and NAP were anticipated to influence variability in release kinetics at an individual module level, due to their different recrystallization tendencies. Fig. 5A shows % RSD in the amount of FEL released at each sampling time point for 3.6 mg modules for FEL5 (green circles) and FEL50 (red circles), with their corresponding drug release profiles in Fig. 5B and 5C, respectively.

For FEL5 and FEL50, drug release from individual modules was within 5% RSD (rounded to the nearest whole number) for the duration of the experiment, except for the start of the release test (t = 10 min for FEL5 and t = 15 min for FEL50). The horizontal dashed lines in Fig. 5A
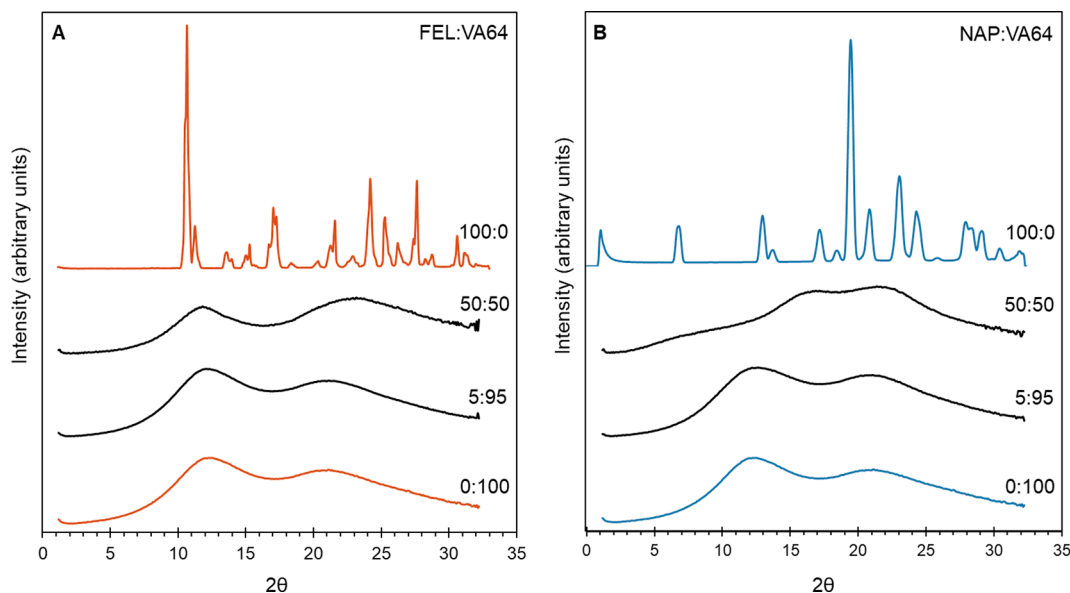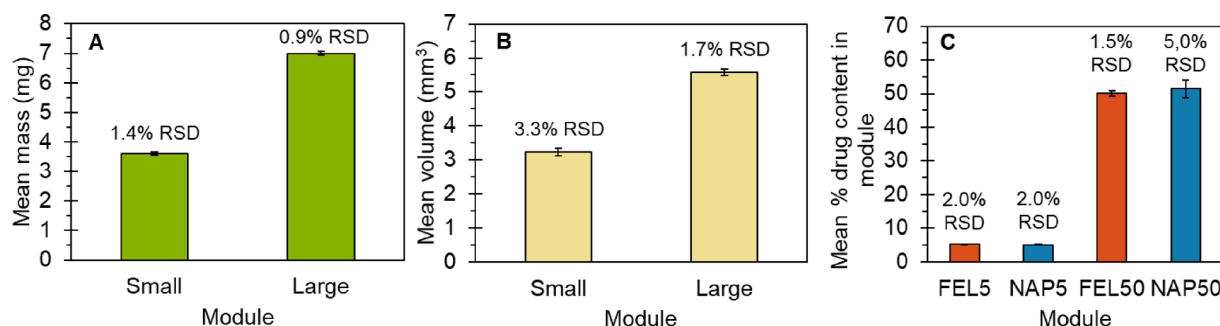

Fig. 3. WAXS curves of (A) FEL and VA64 (red traces), FEL5 and FEL50 (black traces); (B) NAP and VA64 (blue traces), NAP5 and NAP50 (black traces).

Fig. 4. (A) Mean module mass (mg) ± SD of n = 10 modules (small) and n = 15 modules (large); (B) mean module volume (mm³) ± SD of n = 10 modules (small) and n = 15 modules (large); (C) mean % drug content ± SD of n = 5 modules of varying composition. % RSD is indicated above each data point. Note that the small modules include FEL5, FEL50, and NAP50, whereas the large modules include NAP5 and NAP50.
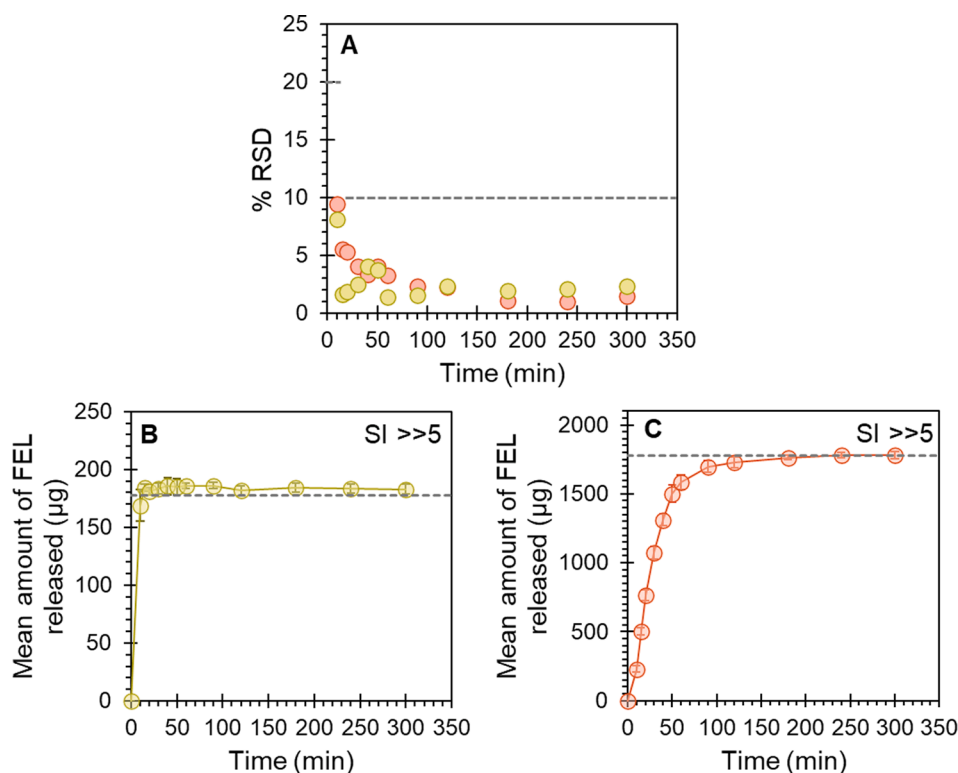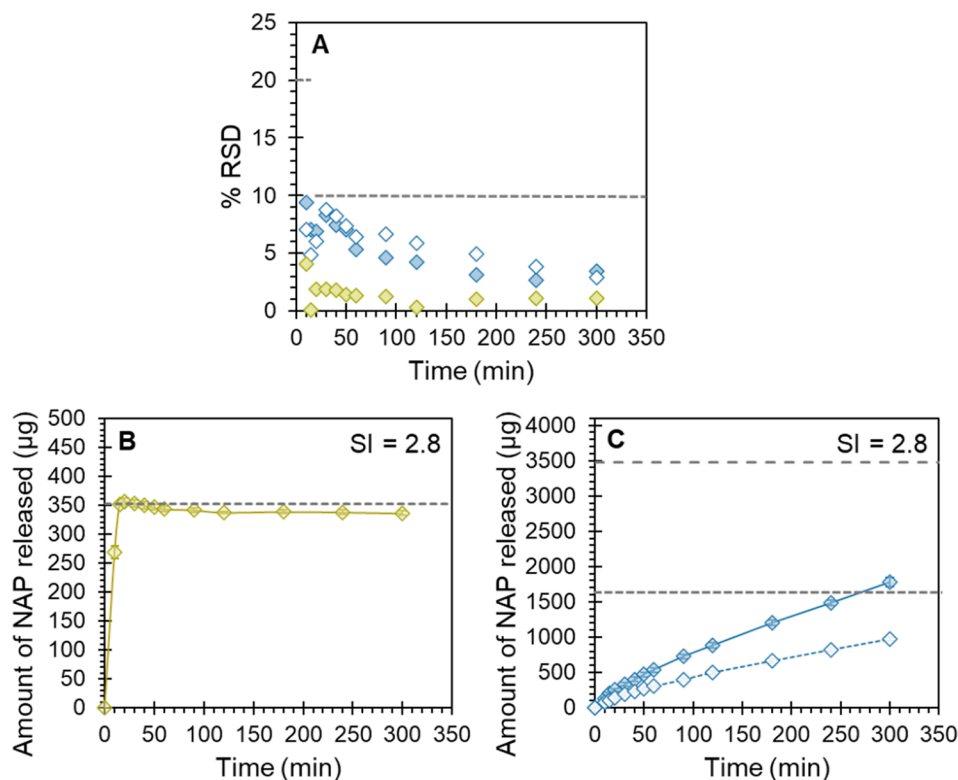

Fig. 5. (A) Variability in the amount of FEL released at each sampling time point from single 3.6 mg modules of FEL5 (green circles) and FEL50 (red circles) and mean amount of FEL released (µg) ± SD of n = 5 samples vs. time from (B) FEL5 and (C) FEL50. The release medium is 0.1 M HCl with 50 mM SDS at 37 °C. The horizontal dashed lines in Fig. 5A denote FDA % RSD limits for immediate release dosage forms and the horizontal dashed lines in Fig. 5B and 5C denote the expected amount of FEL at 100% drug release.

denote acceptable % RSD limits for immediate release dosage forms according to the United States Food and Drug Administration (FDA), with 20% RSD considered acceptable at early time points and 10% RSD considered acceptable for the remaining duration of the drug release test (U.S. Food and Drug Administration, 1997). The European Medicines Agency stipulates a 10% RSD limit throughout the drug release test for prolonged release dosage forms (European Medicines Agency, 2014). In this study, we assumed that the modules should satisfy the same requirements for acceptable variability as dosage forms. However, with future development of modular dosage forms for individualized therapy, clarification of these module specifications is required to determine if they maintain, expand, or reduce, the existing design window. The horizontal dashed lines in Fig. 5B and 5C denote the expected amount of FEL at 100% drug release, revealing that complete drug release was achieved under these test conditions for both FEL5 and FEL50, without subsequent recrystallization in solution. This was expected since it has been shown that the equilibrium solubility of FEL in 1% SDS is 720 µg/mL (Abrahamsson et al., 1994). 1% (50 mM) SDS used in this study therefore created sink conditions with respect to crystalline solubility for

FEL release. In addition to improving the solubility, SDS also improves wetting and dissolution rate (Chen et al., 2018; Garcia-Herrero et al., 2017; Lu et al., 2019). However, upon hydration, crystallization on the surface of the FEL50 modules was observed as a change in optical properties from transparent to opaque within 2 min of exposure to the dissolution medium, which was not observed for the FEL5 modules. Amorphous domains, if present in the solid state, were not sufficiently large to be detected as a separate T_g with DSC. We therefore surmise that this nucleation and crystal growth at the solid–liquid interface occurred due to the increased molecular mobility that accompanies a decline in T_g upon matrix hydration. Supersaturation at the solid–liquid interface has also been previously proposed as a potential explanation for this phenomenon at high drug loads (Edueng, 2019).

The performance of the FEL modules were then compared to that of the NAP modules (Fig. 6). NAP crystalline solubility has been reported as 29.21 µg/mL in 0.1 M HCl at 37 °C (Liu et al., 2017). Addition of 0.5% SDS has previously been shown to result in a five-fold increase in NAP water solubility (Alizadeh et al., 2018). It has also been shown that NAP solubility increases linearly with SDS concentration above the critical

Fig. 6. (A) Variability in the amount of NAP released at each sampling time point from single 7 mg modules of NAP5 (green diamonds), 3.6 mg modules of NAP50 (blue empty diamonds) and 7 mg modules of NAP50 (blue filled diamonds) and mean amount of NAP released(µg) ± SD of n = 5 samples vs. time from (B) NAP5 and (C) NAP50 (blue empty diamonds are 3.6 mg modules and blue filled diamonds are 7 mg modules). The release medium is 0.1 M HCl with 50 mM SDS at 37 °C. The horizontal dashed lines in Fig. 6A denote % RSD limits for immediate release dosage forms according to FDA guidance and the horizontal dashed lines in Fig. 6B and 6C denote the expected amount of NAP at 100% drug release. Variability is smaller than data point when not visible.

micelle concentration at all pHs between pH 2.4 and pH 5.1 (Valero et al., 2020). If this approximation is assumed to apply to the test conditions above, a sink index of 2.8 results for NAP release with 50 mM SDS. Complete drug release was achieved for NAP5 (Fig. 6B) and the small NAP50 modules (Fig. 6C) were confirmed to reach 1817 ± 95 µg NAP released at a 24 h measurement point, corresponding to complete drug release for NAP50. NAP50 therefore reached T50 at 300 min.

Similar to FEL50, a change in NAP50 module optical properties also occurred from transparent to opaque within 5 min of exposure to the dissolution medium. Therefore, recrystallization on the surface of the module occurred upon hydration for both FEL50 and NAP50. Fig. 6A, shows % RSD in NAP release kinetics at an individual module level for NAP5 and NAP50. NAP5 modules exhibited drug release kinetics within 5% RSD throughout the experiment, however, NAP50 demonstrated drug release within 10% RSD, greater variability than the equivalent drug load of FEL. Importantly, the dose fraction in each NAP50 module was within 5% RSD. To determine whether the 7 mg module size was comparable in variability to the 3.6 mg modules sizes used for the FEL modules, NAP50 at a 3.6 mg module size was also evaluated. Fig. 6A shows that no change in % RSD was observed as a result. FEL50 and NAP50 exhibited different drug release rates. Since FEL50 had a greater variability in drug release kinetics at the start of the release test, to account for the varying release rates in FEL50 and NAP50 at a module size of 3.6 mg, % RSD in the amount of drug released was compared at T10 and T40. Fig. 7 shows that FEL50 and NAP50 have comparable variability at similar earlier timepoints in their release profiles.

In contrast to what was expected, differences in the inherent recrystallization tendencies of each API did not impact variability in release kinetics at high drug loads. Altogether, the results under these test conditions indicate that low variability in individual module release kinetics, required for reconfigurability, is obtained at 5% w/w and 50% w/w drug load in individual modules. At a module size of 3.6 mg, this translates to a dose fraction of 180 µg at the lower end (at which fine-tuning of the dose can occur) and up to 1800 µg at the higher end for an individual module. This is a ten-fold range on an individual module level which can be harnessed for the purpose of reconfiguration and
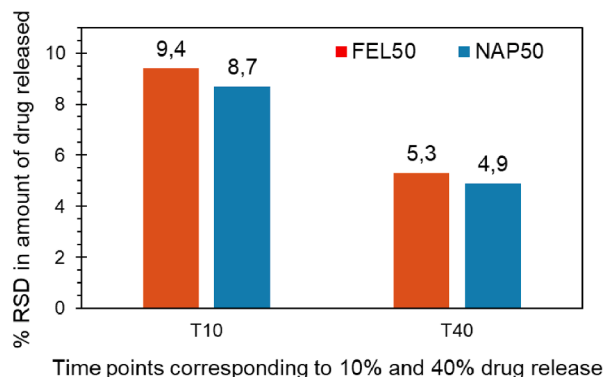

Fig. 7. % RSD in the amount of drug released from FEL50 and NAP50 3.6 mg modules (n = 5) at T10 and T40. The release medium is 0.1 M HCl with 50 mM SDS at 37 °C.

provision of enhanced product variety with reproducible dose and release kinetics. Preliminary investigations of drug release were conducted under non-sink conditions with respect to crystalline solubility without the addition of SDS to the dissolution medium (Fig. 8).

Fig. 8A reveals that amorphization of FEL in FEL5 modules provides a sufficient solubility advantage to allow supersaturation with respect to crystalline solubility. However, this supersaturation was unstable, with subsequent crystallization from the dissolved state occurring rapidly (Fig. 8A). In contrast, even without SDS, under non-sink conditions, supersaturation was achieved and maintained, with complete drug release from NAP5 without the need for SDS. Notably, to obtain an equivalent sink index for FEL5 and NAP5, volumes of the dissolution media were adjusted to remove the influence of their varying crystalline solubilities. This resulted in varying concentrations of VA64, dissolved from the solid dispersion, of 18 µg/mL VA64 and 500 µg/mL VA64, for the FEL5 and NAP5 release tests, respectively. This could play a role in improving the solubility of NAP and/or inhibiting crystallization of
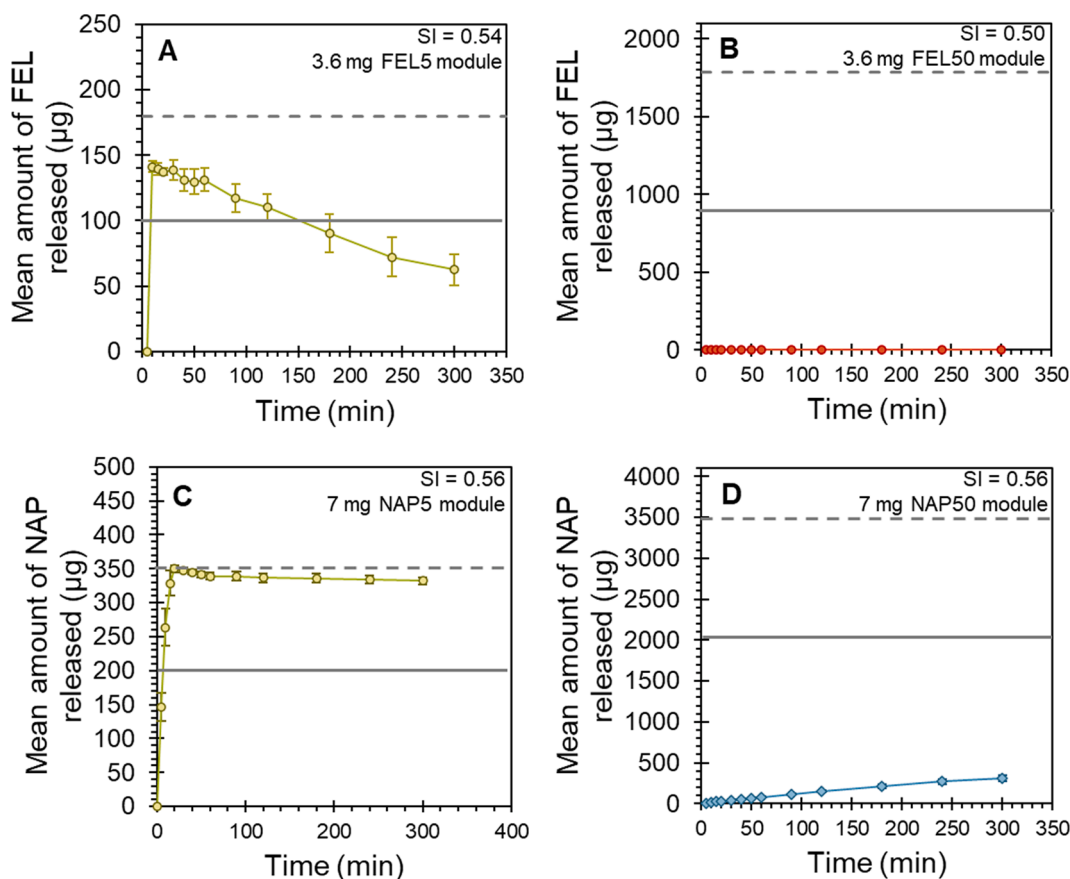
Fig. 8. Mean amount of drug released (μg) ± SD of n = 5 samples vs. time from (A) FEL5 (3.6 mg module), (B) FEL50 (3.6 mg module), (C) NAP5 (7 mg module), and (D) NAP50 (7 mg module). The horizontal dashed lines denote the expected amount of drug at 100% drug release and horizontal solid lines indicate the amount solubilized based on the crystalline solubility of each API. Variability is smaller than data point when not visible.

dissolved NAP from solution. At low drug loads under non-sink conditions, the NAP5 system in this study displays superior performance to FEL5 in exploiting the advantage of the amorphous state, despite the higher recrystallization tendency of NAP. This emphasizes the importance of the ability of the selected polymer to serve as a crystallization inhibitor both in the solid state and during the dissolution.

Drug release from FEL50 under non-sink conditions was not detected for the duration of the experiment without SDS (Fig. 8B). This is in agreement with FEL in VA64 formulations previously investigated (Langham et al., 2012) and was attributed to the observed crystallization on the surface of FEL50 upon hydration. Although crystallization occurred at a different location at high drug loads (in the matrix) compared to low drug loads (in solution), it nonetheless necessitated the inclusion of SDS for robust performance. Recrystallization on the surface of the module also occurred with NAP50, in the absence of SDS, therefore dissolved VA64 (originating from the solid dispersion) could explain the increased solubility of NAP and detectable drug release from NAP50 under non-sink conditions (Fig. 8D).

These results indicate that, at low drug loads, the inherent recrystallization tendency of the drug can be overcome through polymer selection to solubilize and stabilize the drug both in the solid state and in solution (NAP5). Despite drug release from the NAP modules, the lack of FEL release from FEL50 under non-sink conditions did not permit scrutinizing individual module variability in drug release kinetics using test conditions without SDS. Consequently, in this study, individual module FEL and NAP variability in release kinetics were obtained from tests performed with SDS in the dissolution media. Here, the role of SDS was to prevent recrystallization from solution for FEL5 modules at low drug loads and to solubilize crystals that evolved on the surface of the FEL50 and NAP50 modules at high drug loads. Note that in vivo, the

presence of bile could aid in solubilizing the drug and achieving rapid absorption. In future, simultaneous dissolution–absorption studies measuring the absorption potential in relevant gastrointestinal conditions may help elucidate the relationship between solubility, permeability, and dissolution rate for improved clinical applicability.

Both sets of results, with SDS and without SDS, reveal that drug load affects the tendency to recrystallize at the solid–liquid interface upon hydration, regardless of the inherent recrystallization tendency of the drug. Without optimal polymer selection to inhibit this crystallization during storage and throughout dissolution, lower drug loads would be needed for robust dose and release performance, which may hinder applicability to individualized multidrug therapy.

4. Discussion

4.1. Importance of a wide individual module drug loading range for individualized multidrug therapy

It has previously been proposed and demonstrated that, through reconfiguration, enhanced product variety can be achieved cost-effectively from relatively few module variants in a pharmaceutical mass customization context (Siiskonen et al., 2018; Govender et al., 2020a). Fig. 9 illustrates, through exemplification, the difference in product variety achievable through reconfiguration across a narrow drug loading range (middle column) compared to a wider drug loading range (right column). Reconfiguration relies upon unique modules for variety provision therefore the case example with identical modules (left column) is provided as a reference for minimum product variety without reconfiguration.

In both cases with unique modules available to construct a dosage

Fig. 9. Product variety achievable through reconfiguration of unique modules across varying drug loading ranges showing that wide drug loading ranges are desirable to assure enhanced variety through reconfiguration.

form (middle column and right column of Fig. 9), the same number of module variants (three in the examples shown) and the same degree of modularity (three modules in a product in the examples shown) are assumed. The *potential* number of product variants achievable through reconfiguration of unique modules into a dosage form is therefore identical (ten product variants in the example shown). However, when robust individual module performance for dose and release individualization is only assured within a narrow drug loading range, the *actual* number of product variants could be lower than the potential number of product variants. This is due to several combinations yielding the same final product variant. The example in Fig. 9 shows that only seven out of ten possible product variants are achieved within a narrow drug loading range. This scenario also depends on which intermediate drug loads are selected for module variants between modules with the lowest and highest drug loads. In contrast, the column on the right, which represents a wide drug loading range, shows that both the actual and potential number of product variants are ten, fully exploiting the potential of reconfiguration to enhance product variety. Whether or not the differences between each product variant are small enough for fine-tuning to individual needs and large enough for clinically relevant variety provision for individualized therapy remains to be established. For this, the biopharmaceutical performance of these modules under varying conditions in vitro, e.g. (Puppolo et al., 2017), and in vivo, pharmacokinetics and pharmacodynamics, and the translation to clinical effect in individual patients, need to be evaluated. In the context of individualized multidrug therapy, dose and release modifications both play a role in influencing therapeutic outcome based on the individual APIs in the patient's regimen (Alomar, 2014; Moore et al., 2015; Sawada et al., 2003), based on physiological function (Effinger et al., 2019; Lavan and Gallagher, 2016; Stegemann, 2016; Verbeeck and Horsmans, 1998), and based on adherence to therapy (Brown and Bussell, 2011; Burkhart and

Sabate, 2003; Florence and Lee, 2011; Wertheimer et al., 2005), to name a few general examples. Although these could be applicable to FEL and NAP, for the purpose of this study, FEL and NAP were used as model drugs. For future assembly of modules into flexible multidrug dosage forms, the wider the drug loading range at which robust performance is assured for each API module, the greater the flexibility of the multidrug dosage form for individualized multidrug therapy.

4.2. Importance of robust individual module dose and release performance at high drug loadings for individualized multidrug therapy

A key driver for the existence of multidrug dosage forms is the promotion of patient acceptability by reducing pill burdens and simplifying administration. In order to switch from the administration of multiple APIs *via* discrete dosage forms to a single combination dosage form of acceptable size, (Fig. 10), each API in the product should occupy a comparatively lower volume corresponding to its sub-dosage form module size. Yet, the API is still required to span its entire dose range. This is due to the size constraints of pharmaceutical dosage forms intended to be swallowed intact.

Flexible multidrug dosage forms, which facilitate individualization, require an even higher degree of modularity than multidrug dosage forms with fixed dose, fixed release, or interdependent dose, release, and dosage form size. To achieve flexible dosing and/or flexible release for individualization, each API module in the dosage form requires reconfigurable combinations of varying dose and drug release. The API is still required to span its entire clinical dose range despite the progressive reduction in module size in an eventual assembled dosage form for individualized multidrug therapy. Assuming a typical dosage form (e.g. a flat-faced cylindrical tablet with 4 mm height and 8 mm diameter corresponding to 200 mm^3), the module size of 3.2 mm^3 in this study
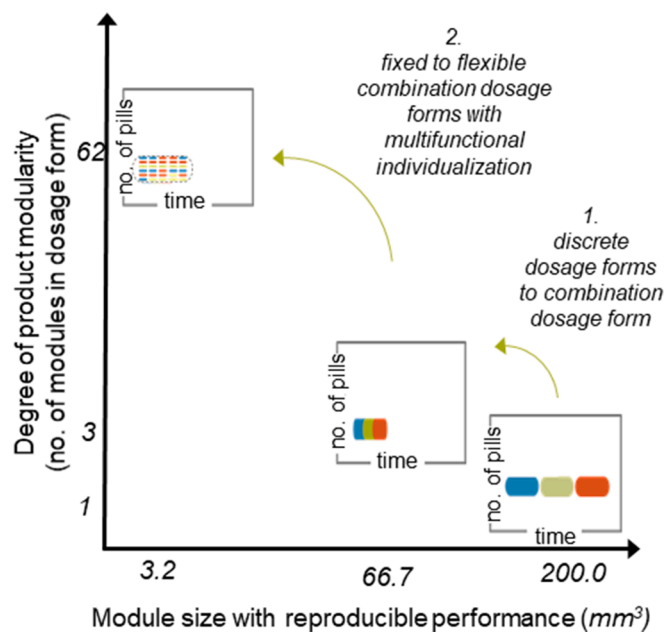
Fig. 10. Design challenges for individualized multidrug therapy that formed the basis of this study involving transitions from discrete to combination dosage forms and from fixed to flexible combination dosage forms with multifunctional individualization. Axes are not to scale.

would allow sixty-two modules to fit within the volumetric constraints of the dosage form, enabling future individualized multidrug therapy from a degree of modularity perspective. However, to access higher combined doses of APIs, it is essential to incorporate higher doses in smaller modules.

Fig. 11 shows that the sixty-two modules that comprise a dosage form in this study can deliver approximately 100 mg of API (50% w/w modules contained 1800 µg API).

This 100 mg represents the sum of doses of all constituent APIs in the multidrug dosage form. The corresponding fixed-dose combination products have the same maximum dose but the requirement for
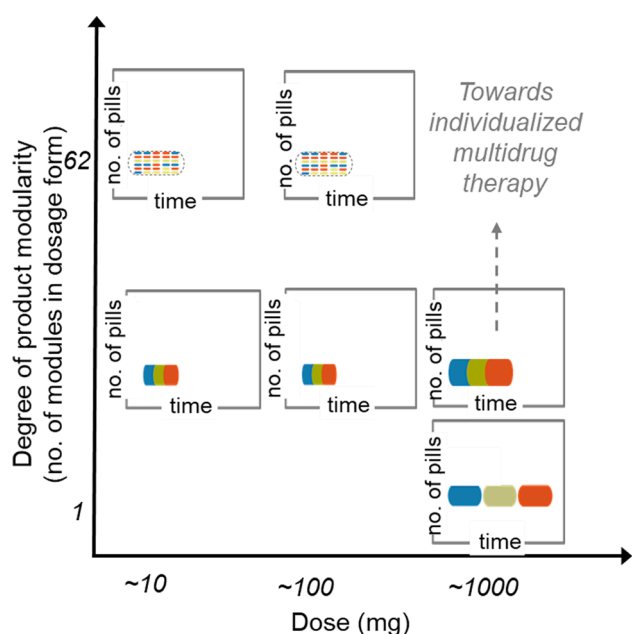

Fig. 11. Degree of product modularity attainable for administration of individualized multidrug therapy at different required doses. Axes are not to scale.

homogeneity at the maximum drug load is inherently stricter for modular dosage forms for individualized multidrug therapy due to smaller modules and an overall higher degree of modularity. This stricter requirement is to enable reproducible individual module dose and release performance for reconfiguration. Fig. 11 shows that, without incorporating higher drug loads within each module, delivering higher doses towards 1000 mg or more either requires an increased size of the multidrug dosage form or reverting to separate administrations. Neither promote patient acceptability, which is a key aspect of individualized therapy, alongside safety and effectiveness. This is true for single drug therapy but is exacerbated for multidrug therapy, even with current mass-produced pharmaceuticals on the market. The greater the number of APIs to be incorporated or the higher the doses of the constituent APIs, the higher the demand for robust performance at higher drug loads and smaller module sizes.

4.3. Summary of requirements for extension of design window based on principal study outcomes

In addition to obtaining robust and reproducible individual module dose and release performance at low and high drug loads and small module sizes, to exploit the advantage of the amorphous state for dissolution rate and bioavailability enhancement, promote clinical relevance, and promote wide applicability of multidrug dosage forms for individualized multidrug therapy, Fig. 12 summarizes the currently satisfied technical criteria for individualized multidrug therapy with poorly water-soluble APIs, based on the systems investigated in this study.

Low variability in dose at low and high drug loads was achieved due to homogeneity in drug content and distribution and high precision in mass and dimensions of individual modules (down to 3.6 mg, 3.2 mm^3 in this study). The former could be attributed mainly to the combined ability of the selected polymeric carrier and the selected melt extrusion processing parameters to completely solubilize the drug in the filament extrudate, resulting in a sufficiently homogeneous drug distribution along the filament at length scales corresponding to individual modules or smaller. Future translation to automated and scalable manufacturing technologies for module generation requires both homogeneous distribution of the drug in the feedstock spanning a wide drug loading range as well as dispensing accuracy and precision for module fabrication. These are the same requirements for reproducible and robust dose and release performance for drugs with high aqueous solubility, so the current design window also includes such drugs. Low drug loads in individual modules define not only the range of the lower limit of the dose range but importantly, throughout the dose range they determine the minimum dose increment which can be used for fine tuning the dose to the needs of individual patients. In this study, at 5% w/w API and a module mass of 3.6 mg, this corresponded to a dose increment of 180 µg. Since drug loads lower than 5% w/w are not expected to adversely alter the homogeneity of drug distribution during melt extrusion (Llusa et al., 2016; Park et al., 2013), it can be anticipated that even lower dose increments towards placebo modules can be achieved in future.

Dose individualization alone is insufficient for individualized therapy, which requires simultaneous tailoring of all the attributes in a dosage form to individual patient needs (Govender et al., 2020a; Govender et al., 2020b). Consequently, a low variability in release kinetics was also demonstrated alongside accuracy and precision in dose at an individual module level at low and high drug loads. Notably, homogeneous distribution of the dose fraction within the module itself (thus at a smaller length scale than the module) is required for reproducible release performance. Not only should this distribution be comparable between modules in the solid state but changes in drug distribution during hydration should also be consistent between modules. Translating this low variability in dose and release performance to robust, clinically relevant performance for poorly soluble APIs requires amorphization in the solid state and a maintained amorphous state
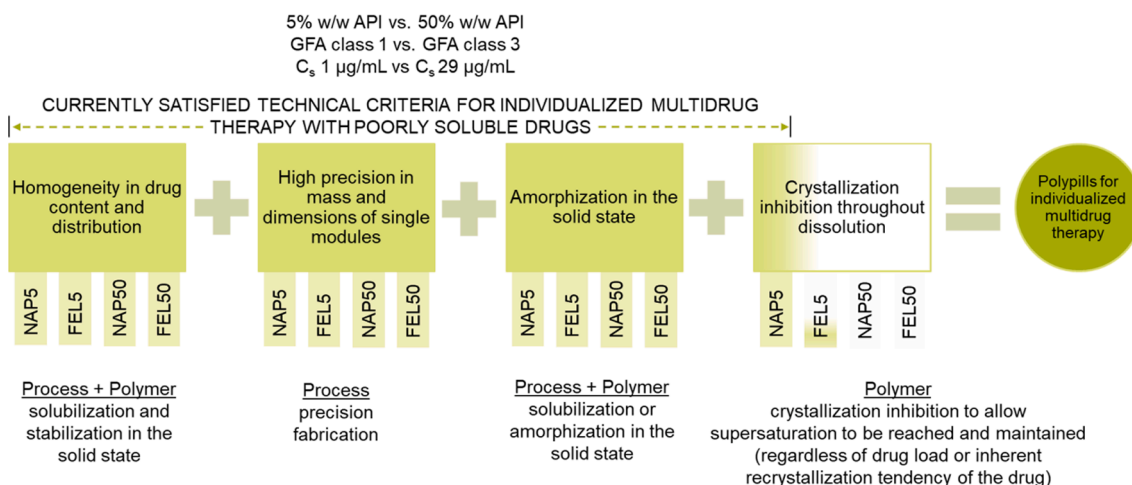
Fig. 12. Summary of the extent to which the technical design requirements for individualized multidrug therapy can currently be achieved for the given compositions in this study (green boxes). Remaining technical requirements to be satisfied (white areas in box on right) form the basis for further extension of the design window. Determinants for each requirement are listed below the shaded boxes.

throughout dissolution (and in vivo uptake) to fully harness the benefits of the amorphous state in bioavailability enhancement and individualization. Amorphization in the solid state was achieved for all compositions due to process and polymer selection to generate amorphous solid dispersions. However, under non-sink conditions, the maintenance of the amorphous state throughout dissolution was only achieved for NAP5, which benefitted from the solubility advantage of the amorphous state and crystallization inhibition by the polymer, allowing supersaturation to be reached and maintained. In contrast, although FEL5 amorphization allowed supersaturation to be achieved, incomplete drug release and the evolution of crystals from solution was attributed to the inability of the polymer (at the concentration use in this study) to stabilize the dissolved FEL. Varying recrystallization tendencies of the APIs did not contribute to variability in dose fractions or drug release kinetics within individual modules across the investigated drug loading range of 5% w/w to 50% w/w API, measured when 50 mM SDS was included in the dissolution medium. In this study, SDS was used to facilitate measurement of variability in release kinetics between modules. For some drugs, SDS inclusion in the dissolution medium is recommended to improve performance and simulate certain in vivo conditions. However, in the specific case of individualized multidrug therapy, an API's reliance on SDS for optimal performance could influence the performance of other APIs intended to be included the multidrug dosage form. This could restrict the applicability of multidrug dosage forms further to systems that perform comparably with or without SDS e.g. NAP5 in this study. Crystallization in the solid state upon hydration (NAP50 and FEL50) and crystallization from solution (FEL5) emphasize that polymer selection for crystallization inhibition in the solid state and solution is a key determinant in extending the applicability of multidrug dosage forms towards individualized multidrug therapy with poorly water-soluble APIs.

5. Conclusions

Enabling individualized multidrug therapy with modular dosage forms is accompanied by stricter requirements on accuracy and precision of the dose and robustness in release kinetics due to the small size of modules in multidrug dosage forms for individualization. The demand for higher drug loads at smaller module sizes could impact drug distribution, dose, and release kinetics. On the length scale of an individual module, this study has demonstrated that reproducible dose and release performance was achieved both at a wide drug loading range and at a small module size. This is critical to obtain the desired degree of modularity for individualization and for simplified administration of

multidrug therapy as multidrug dosage forms upon future assembly of modules.

This study expanded the current design window for poorly water-soluble drugs by demonstrating reproducible individual module dose and release performance with poorly water-soluble APIs with different physicochemical characteristics. This demonstration supports future assembly of modules into multidrug dosage forms for individualized multidrug therapy, where applicability to a broader range of APIs and interchangeability between APIs to suit diverse individual therapeutic regimens can be achieved. Regardless of drug load, API recrystallization tendency did not impact the attainment of accurate and precise dose fractions or reproducible release kinetics in 3.6 mg ($\sim$3.2 mm^3) modules. In fact, despite the higher inherent recrystallization tendency of NAP, it exhibited superior performance to FEL at low drug loads due to amorphization and stabilization of the drug in solution by the polymer. Polymer selection was deemed to be of primary importance to expanding the design window (over the dose and inherent recrystallization tendency of the API).

Requirements for individualized multidrug therapy applicable to APIs with poor aqueous solubility complements the research trajectory in the field of amorphous solid dispersions with regards to the need for incorporation of higher drug loads with robust performance (Dedroog et al., 2019; Lu et al., 2019; Tian et al., 2020). For individualized therapy, this performance should be assured at the size of the modules comprising a dosage form. Our study outcomes make a strong case in favour of interdisciplinary research for individual patient benefit to be maximized. Importantly, progress towards the goal of improved performance at higher drug loads will not only improve dosage form performance for conventional single drug therapy with poorly soluble APIs but also represents a key missing puzzle piece in realizing individualized multidrug therapy for a wider variety of APIs.

CRediT authorship contribution statement

Rydvikha Govender: Conceptualization, Methodology, Validation, Formal analysis, Investigation, Writing - original draft, Writing - review & editing, Visualization, Project administration. **Susanna Abrahmsén-Alami:** Methodology, Writing - review & editing, Supervision. **Staffan Folestad:** Conceptualization, Writing - review & editing, Supervision. **Martina Olsson:** Methodology, Formal analysis, Investigation, Writing - review & editing. **Anette Larsson:** Methodology, Writing - review & editing, Supervision.

Declaration of Competing Interest

Acknowledgements

Funding

Appendix A. Supplementary material

Supplementary data to this article can be found online at https://doi.org/10.1016/j.ijpharm.2021.120625.

References

Abrahamsson, Bertil, Johansson, Dick, Torstensson, Arne, Wingstrand, Karin, 1994. Evaluation of solubilizers in the drug release testing of hydrophilic matrix extended-release tablets of felodipine. Pharm. Res. 11, 1093–1097.

Acosta-Vélez, G.F., Linsley, C.S., Zhu, T.Z., Wu, W., Wu, B.M., 2018. Photocurable bioinks for the 3D pharming of combination therapies. Polymers 10.

Alhalaweh, A., Alzghoul, A., Kaialy, W., Mahlin, D., Bergstrom, C.A., 2014. Computational predictions of glass-forming ability and crystallization tendency of drug molecules. Mol Pharm 11, 3123–3132.

Alizadeh, M.N., Shayanfar, A., Jouyban, A., 2018. Solubilization of drugs using sodium lauryl sulfate: Experimental data and modeling. J. Mol. Liq. 268, 410–414.

Alomar, M.J., 2014. Factors affecting the development of adverse drug reactions (Review article). Saudi Pharm J 22, 83–94.

Bangalore, S., Kamalakkannan, G., Parkar, S., Messerli, F.H., 2007. Fixed-dose combinations improve medication compliance: a meta-analysis. Am J Med 120, 713–719.

Baumgartner, A., Drame, K., Geutjens, S., Airaksinen, M., 2020. Does the polypill improve patient adherence compared to its individual formulations? A systematic review. Pharmaceutics 12. https://doi.org/10.3390/pharmaceutics12020190.

Bhatia, S., Kumar, B., Mittal, S., 2014. Oral Chronotherapeutics: Future of Drug Delivery Systems. Int. J. Sci. Study 2, 55–58.

Brown, M.T., Bussell, J.K., 2011. Medication adherence: WHO cares? Mayo Clin Proc 86, 304–314.

Burkhart, P.V., Sabate, E., 2003. Adherence to long-term therapies: Evidence for action. J Nurs Scholarship 35.

Chen, J., Chen, Y., Huang, W., Wang, H., Du, Y., Xiong, S., 2018. Bottom-Up and Top-Down Approaches to Explore Sodium Dodecyl Sulfate and Soluplus on the Crystallization Inhibition and Dissolution of Felodipine Extrudates. J Pharm Sci 107, 2366–2376.

De Luca, M., Ioele, G., Ragno, G., 2019. 1,4-Dihydropyridine Antihypertensive Drugs: Recent Advances in Photostabilization Strategies. Pharmaceutics 11.

Dedroog, S., Huygens, C., Van den Mooter, G., 2019. Chemically identical but physically different: A comparison of spray drying, hot melt extrusion and cryo-milling for the formulation of high drug loaded amorphous solid dispersions of naproxen. Eur J Pharm Biopharm 135, 1–12.

Demiri, V., Stranzinger, S., Rinner, P., Piller, M., Sacher, S., Lingitz, J., Khinast, J., Salar-Behzadi, S., 2018. Gluing Pills Technology: A novel route to multilayer tablet manufacturing. Int J Pharm 548, 672–681.

Deng, J., Vozmediano, V., Rodriguez, M., Cavallari, L.H., Schmidt, S., 2017. Genotype-guided dosing of warfarin through modeling and simulation. Eur J Pharm Sci 109S, S9–S14.

Drumond, N., Stegemann, S., 2020. Better Medicines for Older Patients: Considerations between Patient Characteristics and Solid Oral Dosage Form Designs to Improve Swallowing Experience. Pharmaceutics 13.

Edueng, K., 2019. Molecular Mechanisms Influencing the Performance of Amorphous Formulations for Poorly Water-Soluble Drugs. Uppsala University, Digital Comprehensive Summaries of Uppsala Dissertations from the Faculty of Pharmacy, p. 276. https://www.dissertations.se/dissertation/516e4bfba5/.

Effinger, A., O'Driscoll, C.M., McAllister, M., Fotaki, N., 2019. Impact of gastrointestinal disease states on oral drug absorption - implications for formulation design - a PEARRL review. J Pharm Pharmacol 71, 674–698.

European Medicines Agency, 2014. Guideline on quality of oral modified release products. In: (CHMP), Committee for Medicinal Products for Human Use (Ed.). European Medicines Agency, London, United Kingdom, p. 8. https://www.ema.europa.eu/en/documents/scientific-guideline/guideline-quality-oral-modified-release-products_en.pdf.

Fernandez-Garcia, R., Prada, M., Bolas-Fernandez, F., Ballesteros, M.P., Serrano, D.R., 2020. Oral Fixed-Dose Combination Pharmaceutical Products: Industrial Manufacturing Versus Personalized 3D Printing. Pharm Res 37, 132.

Ferrendelli, J.A., 2001. Concerns with antiepileptic drug initiation: safety, tolerability, and efficacy. Epilepsia 42 (Suppl 4), 28–30.

Florence, A.T., Lee, V.H., 2011. Personalised medicines: more tailored drugs, more tailored delivery. Int J Pharm 415, 29–33.

Fuenmayor, E., O'Donnell, C., Gately, N., Doran, P., Devine, D.M., Lyons, J.G., McConville, C., Major, I., 2019. Mass-customization of oral tablets via the combination of 3D printing and injection molding. Int J Pharm 569, 118611.

Garcia-Herrero, V., Torrado, C., Garcia-Rodriguez, J.J., Lopez-Sanchez, A., Torrado, S., Torrado-Santiago, S., 2017. Improvement of the surface hydrophilic properties of naproxen particles with addition of hydroxypropylmethyl cellulose and sodium dodecyl sulphate: In vitro and in vivo studies. Int J Pharm 529, 381–390.

Genina, N., Boetker, J.P., Colombo, S., Harmankaya, N., Rantanen, J., Bohr, A., 2017. Anti-tuberculosis drug combination for controlled oral delivery using 3D printed compartmental dosage forms: From drug product design to in vivo testing. J Control Release 268, 40–48.

Gershenson, J.K., Prasad, G.J., Allamneni, S., 1999. Modular Product Design: A Life-Cycle View. J. Integr. Des. Process Sci. 3, 13–26.

Govender, R., Abrahmsen-Alami, S., Folestad, S., Larsson, A., 2019. High Content Solid Dispersions for Dose Window Extension: A Basis for Design Flexibility in Fused Deposition Modelling. Pharm Res 37, 9.

Govender, R., Abrahmsen-Alami, S., Larsson, A., Borde, A., Liljeblad, A., Folestad, S., 2020a. Independent Tailoring of Dose and Drug Release via a Modularized Product Design Concept for Mass Customization. Pharmaceutics 12.

Govender, R., Abrahmsen-Alami, S., Larsson, A., Folestad, S., 2020b. Therapy for the individual: Towards patient integration into the manufacturing and provision of pharmaceuticals. Eur J Pharm Biopharm 149, 58–76.

Guo, W., Li, C., Du, P., Wang, Y., Zhao, S., Wang, J., Yang, C., 2020. Thermal properties of drug polymorphs: A case study with felodipine form I and form IV. Journal of Saudi Chemical Society 24, 474–483.

Hens, B., Corsetti, M., Spiller, R., Marciani, L., Vanuytsel, T., Tack, J., Talattof, A., Amidon, G.L., Koziolek, M., Weitschies, W., Wilson, C.G., Bennink, R.J., Brouwers, J., Augustijns, P., 2017. Exploring gastrointestinal variables affecting drug and formulation behavior: Methodologies, challenges and opportunities. Int J Pharm 519, 79–97.

Kawakami, K., 2019. Crystallization Tendency of Pharmaceutical Glasses: Relevance to Compound Properties, Impact of Formulation Process, and Implications for Design of Amorphous Solid Dispersions. Pharmaceutics 11.

Khaled, S.A., Burley, J.C., Alexander, M.R., Yang, J., Roberts, C.J., 2015a. 3D printing of five-in-one dose combination polypill with defined immediate and sustained release profiles. J Control Release 217, 308–314.

Khaled, S.A., Burley, J.C., Alexander, M.R., Yang, J., Roberts, C.J., 2015b. 3D printing of tablets containing multiple drugs with defined release profiles. Int J Pharm 494, 643–650.

Konno, H., Taylor, L.S., 2006. Influence of different polymers on the crystallization tendency of molecularly dispersed amorphous felodipine. J Pharm Sci 95, 2692–2705.

Langham, Z.A., Booth, J., Hughes, L.P., Reynolds, G.K., Wren, S.A., 2012. Mechanistic insights into the dissolution of spray-dried amorphous solid dispersions. J Pharm Sci 101, 2798–2810.

Laukamp, E.J., Knop, K., Thommes, M., Breitkreutz, J., 2016. Micropellet-loaded rods with dose-independent sustained release properties for individual dosing via the Solid Dosage Pen. Int J Pharm 499, 271–279.

Lavan, A.H., Gallagher, P., 2016. Predicting risk of adverse drug reactions in older adults. Ther Adv Drug Saf 7 (1), 11–22.

Lehmkemper, K., Kyeremateng, S.O., Bartels, M., Degenhardt, M., Sadowski, G., 2018. Physical stability of API/polymer-blend amorphous solid dispersions. Eur J Pharm Biopharm 124, 147–157.

Liu, X., Zhou, L., Zhang, F., 2017. Reactive Melt Extrusion To Improve the Dissolution Performance and Physical Stability of Naproxen Amorphous Solid Dispersions. Mol Pharm 14, 658–673.

Llusa, M., Mohr, S., Baumgartner, R., Paudel, A., Koscher, G., Khinast, J., 2016. Continuous low-dose feeding of highly active pharmaceutical ingredients in hot-melt extrusion. Drug Dev Ind Pharm 42, 1360–1364.

Lu, Y., Chen, J., Yi, S., Xiong, S., 2019. Enhanced felodipine dissolution from high drug loading amorphous solid dispersions with PVP/VA and sodium dodecyl sulfate. J. Drug Delivery Sci. Technol. 53.

Maddineni, S., Battu, S.K., Morott, J., Majumdar, S., Murthy, S.N., Repka, M.A., 2015. Influence of process and formulation parameters on dissolution and stability characteristics of Kollidon(R) VA 64 hot-melt extrudates. AAPS PharmSciTech 16, 444–454.

McConnell, E.L., Fadda, H.M., Basit, A.W., 2008. Gut instincts: explorations in intestinal physiology and drug delivery. Int J Pharm 364, 213–226.

Meltzer, E.O., Welch, M.J., Ostrom, N.K., 2006. Pill swallowing ability and training in children 6–11 years of age. Clin. Pediatr. 45, 725–733.

Messina, R., Becker, R., van Riet-Nales, D.A., Stegemann, S., 2015. Results from a preliminary review of scientific evidence for appropriateness of preparations, dosage forms and other product design elements for older adult patients. Int J Pharm 478, 822–828.

Moore, N., Pollack, C., Butkerait, P., 2015. Adverse drug reactions and drug-drug interactions with over-the-counter NSAIDs. Ther Clin Risk Manag 11, 1061–1075.

Nidanapu, R.P., Rajan, S., Mahadevan, S., Gitanjali, B., 2016. Tablet Splitting of Antiepileptic Drugs in Pediatric Epilepsy: Potential Effect on Plasma Drug Concentrations. Paediatr Drugs 18, 451–463.

Page, S., Coupe, A., Barrett, A., 2016. An industrial perspective on the design and development of medicines for older patients. Int J Pharm 512, 352–354.

Palazi, E., Karavas, E., Barmpalexis, P., Kostoglou, M., Nanaki, S., Christodoulou, E., Bikiaris, D.N., 2018. Melt extrusion process for adjusting drug release of poorly water soluble drug felodipine using different polymer matrices. Eur J Pharm Sci 114, 332–345.

Panini, P., Rampazzo, M., Singh, A., Vanhoutte, F., Van den Mooter, G., 2019. Myth or Truth: The Glass Forming Ability Class III Drugs Will Always Form Single-Phase Homogenous Amorphous Solid Dispersion Formulations. Pharmaceutics 11.

Park, J.B., Kang, C.Y., Kang, W.S., Choi, H.G., Han, H.K., Lee, B.J., 2013. New investigation of distribution imaging and content uniformity of very low dose drugs using hot-melt extrusion method. Int J Pharm 458, 245–253.

Pereira, B.C., Isreb, A., Forbes, R.T., Dores, F., Habashy, R., Petit, J.B., Alhnan, M.A., Oga, E.F., 2019. 'Temporary Plasticiser': A novel solution to fabricate 3D printed patient-centred cardiovascular 'Polypill' architectures. Eur J Pharm Biopharm 135, 94–103.

Pereira, B.C., Isreb, A., Isreb, M., Forbes, R.T., Oga, E.F., Alhnan, M.A., 2020a. Additive Manufacturing of a Point-of-Care "Polypill:" Fabrication of Concept Capsules of Complex Geometry with Bespoke Release against Cardiovascular Disease. Adv Healthc Mater 9, e2000236.

Pereira, B.C., Isreb, A., Isreb, M., Forbes, R.T., Oga, E.F., Alhnan, M.A., 2020b. Additive Manufacturing of a Point-of-Care "Polypill:" Fabrication of Concept Capsules of Complex Geometry with Bespoke Release against Cardiovascular Disease. Adv. Healthcare Mater. 9.

Pizarro, N., Günther, G., Núñez-Vergara, L.J., 2007. Photophysical and photochemical behavior of nimodipine and felodipine. J. Photochem. Photobiol., A 189, 23–29.

Pouplin, T., Phuong, P.N., Toi, P.V., Nguyen Pouplin, J., Farrar, J., 2014. Isoniazid, pyrazinamide and rifampicin content variation in split fixed-dose combination tablets. PLoS ONE 9, e102047.

Puppolo, M.M., Hughey, J.R., Dillon, T., Storey, D., Jansen-Varnum, S., 2017. Biomimetic Dissolution: A Tool to Predict Amorphous Solid Dispersion Performance. AAPS PharmSciTech 18, 2841–2853.

Ranmal, S.R., Cram, A., Tuleu, C., 2016. Age-appropriate and acceptable paediatric dosage forms: Insights into end-user perceptions, preferences and practices from the Children's Acceptability of Oral Formulations (CALF) Study. Int J Pharm 514, 296–307.

Robles-Martinez, P., Xu, X., Trenfield, S.J., Awad, A., Goyanes, A., Telford, R., Basit, A. W., Gaisford, S., 2019. 3D printing of a multi-layered polypill containing six drugs using a novel stereolithographic method. Pharmaceutics 11.

Rosenthal, T., Gavras, I., 2006. Fixed-Drug Combinations as First-Line Treatment for Hypertension. Prog. Cardiovasc. Dis. 48, 416–425.

Sadia, M., Isreb, A., Abbadi, I., Isreb, M., Aziz, D., Selo, A., Timmins, P., Alhnan, M.A., 2018. From 'fixed dose combinations' to 'a dynamic dose combiner': 3D printed bilayer antihypertensive tablets. Eur J Pharm Sci 123, 484–494.

Sarpal, K., Delaney, S., Zhang, G.G.Z., Munson, E.J., 2019. Phase Behavior of Amorphous Solid Dispersions of Felodipine: Homogeneity and Drug-Polymer Interactions. Mol Pharm 16, 4836–4851.

Sawada, T., Sako, K., Yoshihara, K., Nakamura, K., Yokohama, S., Hayashi, M., 2003. Timed-Release Formulation to Avoid Drug-Drug Interaction between Diltiazem and Midazolam. J Pharm Sci-Us 92, 790–797.

Siiskonen, M., Folestad, S., Malmqvist, J., 2018. Applying Function-Means Tree Modelling to Personalized Medicines, NordDesign 2018. Linköping, Sweden. https ://research.chalmers.se/en/publication/508003.

Smeets, A., Re, I.L., Clasen, C., Van den Mooter, G., 2020. Fixed dose combinations for cardiovascular treatment via coaxial electrospraying: Coated amorphous solid dispersion particles. Int J Pharm 577, 118949.

Song, Y., Wang, L., Yang, P., Wenslow Jr., R.M., Tan, B., Zhang, H., Deng, Z., 2013. Physicochemical characterization of felodipine-kollidon VA64 amorphous solid dispersions prepared by hot-melt extrusion. J Pharm Sci 102, 1915–1923.

Srai, J.S., Harrington, T., Alinaghian, L., Phillips, M., 2015. Evaluating the potential for the continuous processing of pharmaceutical products—a supply network perspective. Chem. Eng. Process. Process Intensif. 97, 248–258.

Stegemann, S., 2016. Developing Drug Products in an Aging Society: From Concept to Prescribing. Springer, AAPS Press.

Stegemann, S., Gosch, M., Breitkreutz, J., 2012. Swallowing dysfunction and dysphagia is an unrecognized challenge for oral drug therapy. Int J Pharm 430, 197–206.

Sun, D.D., Wen, H., Taylor, L.S., 2016. Non-Sink Dissolution Conditions for Predicting Product Quality and In Vivo Performance of Supersaturating Drug Delivery Systems. J Pharm Sci 105, 2477–2488.

Tian, Y., Jacobs, E., Jones, D.S., McCoy, C.P., Wu, H., Andrews, G.P., 2020. The design and development of high drug loading amorphous solid dispersion for hot-melt extrusion platform. Int J Pharm 586, 119545.

U.S. Food and Drug Administration, 1997. Guidance for Industry: Dissolution Testing of Immediate Release Solid Oral Dosage Forms, Immediate Release Expert Working Group of the Biopharmaceutics Coordinating Committee and Center for Drug Evaluation and Research. In: Food and Drug Administration (Ed.). Maryland, United States, p. 9. https://www.fda.gov/media/70936/download.

Ulrich, K., Tung, K., 1991. In: Fundamentals of product modularity. Proceedings of the 1991 ASME Winter Annual Meeting Symposium on Issues in Design/Manufacturing Integration. https://link.springer.com/content/pdf/10.1007/978-94-011-1390 -8_12.pdf.

Valero, M., Sultimova, N.B., Houston, J.E., Levin, P.P., 2020. Naproxen sodium salt photochemistry in aqueous sodium dodecyl sulfate (SDS) ellipsoidal micelles. J. Mol. Liq.

Verbeeck, R.K., Horsmans, Y., 1998. Effect of hepatic insufficiency on pharmacokinetics and drug dosing. Pharm World Sci 20, 183–192.

Wening, K., Breitkreutz, J., 2011. Oral drug delivery in personalized medicine: unmet needs and novel approaches. Int J Pharm 404, 1–9.

Wertheimer, A.I., Santella, T.M., Finestone, A.J., Levy, R.A., 2005. Drug Delivery Systems Improve Pharmaceutical Profile and Facilitate Medication Adherence. Advances in Therapy 22, 559–577.

Wilson, M.W., 2016. Manufacturing Platforms for Patient-Centric Drug Products. In: Stegemann, S. (Ed.), Developing Drug Products in an Aging Society. Springer, pp. 447–483.